A Hardware Based Implementation of a Tactile Sensory System For Neuromorphic Signal Processing Applications

M. Pearson*, M. Nibouche*, I. Gilhespy*, K. Gurney♦, C. Melhuish*, B. Mitchinson♦, A.G. Pipe*
{martin.pearson, mokhtar.nibouche, ian.gilhespy, chris.melhuish, anthony.pipe}@uwe.ac.uk
* Bristol Robotics Laboratory, University of the West of England, Bristol BS16 1QY, UK
{k.gurney, b.mitchinson}@sheffield.ac.uk
♦ Adaptive Behaviour Research Group, University of Sheffield, Sheffield S10 2TP, UK

ABSTRACT

The implementation of a tactile sensory system for neuromorphic signal processing applications is presented. It has been developed by modelling the structure and behaviour of real rodent facial vibrissae. The primary afferents have been modelled using empirical data taken from electrophysiological measurements, and implemented in real time using hardware processors (DSP/FPGA). Pipelining techniques were employed to maximise the utility of the FPGA hardware. The system is to be integrated into a more complete whisker sensory model, including neural structures within the central nervous system, which can be used to orientate a mobile robot.

1. INTRODUCTION

The rodent family of mammals have the ability to orientate rapidly through confined, dark and visually occluded environments, as well as to discriminate differences in fine surface textures [1]. This highly sophisticated capability is largely due to a very advanced tactile based sensory system derived from their facial vibrissae (array of whiskers). A part of the work undertaken in Whiskerbot [2], a collaborative project involving both EE engineers and neuroscientists, is to establish a model of the rodent whisker sensory system using a predominantly bio-mimetic approach. This includes the modelling of both the bio-mechanics of the vibrissae itself and the underlying neural pathways, structures and processing algorithms of the peripheral and central nervous system (CNS). The model accepts as inputs analogue signals caused by the deflection of the whiskers and generates train of spikes to be fed to the brainstem. The lower brain (brainstem) has already been FPGA modelled using a neuromorphic approach [3]. The developed sensory model is to be ultimately embedded in a mobile robot platform, which will operate in a real world environment, utilising the artificial whisker sensory array to enact behaviours analogous to active rodents, such as wall following, object recognition and surface textural discrimination.

The approach proposed in this work differs markedly from previous whisker based robotic sensor systems [4][5], which adopted a more abstract engineered interpretation of the whiskers. In this paper a more biologically inspired approach has been taken, adopting instead a philosophy much more akin to the `Brain Based Device' approach [6]. Also, in the design of the artificial vibrissae, the characteristic curvature and tapering observed in real rodent have been included. Two pairs of diametrically opposing micro strain gauges were bonded to the periphery at the base of the artificial vibrissae. The configuration of the gauges is such that deflections of the vibrissal shaft, when clamped at the base, will generate a proportional two dimensional strain measurement vector (see [7] for details). This differs from [8] as we intend to explore the role of vibrissae deflections in both planes. We also wish to measure the `DC' component of vibrissae deflections which is not possible using the electret microphone system of Amouse [9].

The paper is organised as follows: in section 2, a brief description of the vibrissae is given prior to the introduction of both the mechanical and the mechanoreceptor models. The real time hardware implementation is presented and described in details in section 3. Section 4 is dedicated to the results and discussion. Finally a conclusion closes the work.

2. MODELS

2.1 Background

The vibrissae of a rodent can be broadly classified into 2 classes; micro and macro [10]. They represent (vibrissae) the visible `front end' of an advanced sensory system which involves the interaction of numerous neural structures throughout the CNS of the animal [11]. Ultimately the mechanical deformations of the vibrissal shaft, as it interacts with the environment, are translated into information, which the CNS can interpret and upon which generate appropriate action selections. It has been proposed that the two species of vibrissae contribute different specialist functionality to the sensor array [10]. It has also been demonstrated that the macro vibrissae are independently capable of discriminating relatively fine textural features as well as detecting object proximity and determining gross shape [10]. This multi functionality, and the simple fact of their larger physical size, led us to model only the micro vibrissae in our initial prototype as illustrated in Figure 1.

2.2 The Follicle Sinus Complex (FSC) Model

Each of the vibrissae of a rodent originates from a sinus in the skin of the mystacial pad, in which, is a structure that encapsulates the base of the vibrissae called the follicle consisting of a number of complex sub-structures. Situated within these sub-structures are large numbers of cells which are sensitive to mechanical deformation, hence called mechanoreceptors. There are a variety of species of mechanoreceptor found in the follicle which in turn excite the Primary Afferents (PAs) which innervate the follicle. A principle classification metric for these PAs is how rapidly they adapt to stimuli. PAs that rapidly adapt to the stimulus are consequently classified as Rapidly Adapting (RA), where as the others are Slowly Adapting (SA).

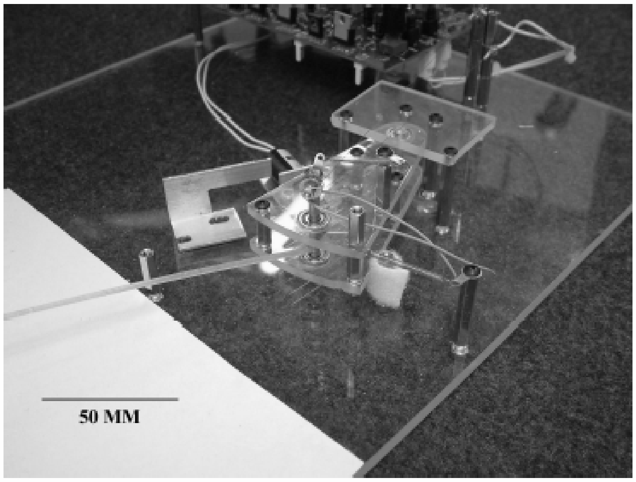

Figure 1: Whisker prototype.

2.3 The Mechanical Model

Two types of PA have been modelled to represent the two extremes of the adaptation behaviours. The mechanoreceptors, which excite the PAs, are located at different depths within the follicle which consists of solid membranes encapsulating elastic sheaths. The location of the cells within the follicle will effect how the mechanical deformations of the Vibrissal Shaft are translated. This mechanical differentiation has been modelled using an analogous network of mass-spring-dampers, the strain in the springs between rigid sub-follicle membranes representing the mechanical force experienced by the mechanoreceptor.

2.4 The Mechanoreceptor Model

The mechanoreceptor models themselves are simplified functional representations of large groups of actual cells. Indeed what are actually being modelled are the PAs that are excited by the mechanoreceptors, translating this excitation in the form of spike trains to brainstem. However, for clarity we refer to a single model as a single mechanoreceptor of a particular species with an associated Most Effective Angle (MEA) of sensitivity to the direction of mechanical deformations in the vibrissal shaft. When the vibrissae bends in a certain direction, the mechanoreceptors with MEAs 180^{o} to the direction of bend, will become maximally excited due to the pivot point at the sinus. This directional sensitivity has been modelled along with a number of other features, as it is being illustrated in Figure 2 (see also [12]).

3. DSP/FPGA BASED IMPLEMENTATION

3.1 FSC Model Reduction

Initially, the FSC was developed and implemented using software packages and a desktop Personal Computer (PC). To translate this model into an embedded solution required us to adopt a number of constraints and further model simplifications. The integration period of the software model was approximately 1μS, i.e., an update rate of 1MHz. The number of mechanoreceptors modelled was in the region of one hundred per follicle utilising a number of computationally expensive mathematical software functions, all implemented using floating point arithmetic. Simulations of the model by the biologists using a reduced update rate revealed that an acceptable amount of model degradation was experienced with update rates as low as 10 KHz. The computationally expensive operation of updating the mass-spring-damper based mechanical model of the FSC was reduced to a pair of second order Infinite Impulse Response (IIR) filters. The two filters represent the mechanical translation of the vibrissae induced deformation of the follicle on either side of a glassy membrane. The number of mechanoreceptors which have been modelled in the embedded system was initially arbitrarily chosen as 40 per follicle. This figure was later found to be almost optimal with regards to the maximum number that could be modelled in real-time by the system. The MEAs of the mechanoreceptors could be uniformly distributed around the follicle or, as is the case in the biology, be concentrated, thereby creating regions of increased sensitivity for vibrissal displacements of specific orientations.

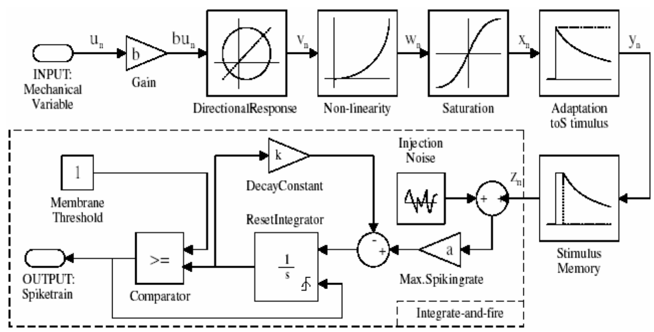

Figure 2: Block diagram of the mechanoreceptor model [12]

3.2 Development

The TMS320C28x series of Texas Instruments DSP processors were initially chosen to implement the FSC and mechanoreceptor models as they have the advantage of on-chip peripheral modules such as an Analogue to Digital Converter (ADC), high speed Serial Peripheral Interface (SPI) and 2 EVent managers (EV) for real-time synchronous performance. This kind of processor has a modified Harvard architecture with dual data and instruction buses for high speed processing. They do not have a hardware floating point unit so floating point arithmetic requires the use of computationally expensive software solutions. For this reason a fixed point number system was adopted using appropriate scaling where necessary to reduce the quantisation distortion that is introduced. Preliminary experiments and calculations revealed that the processing performance of the DSP was inadequate to meet the required specification. Each DSP was required to sample and subsequently model the FSC and mechanoreceptors of 6 vibrissa, (one DSP per sensor chassis, every 100 μS). Instead of distributing the processing between multiple DSPs on each chassis, which increases communications and PCB design overheads, we added a single Field Programmable Gate Array (FPGA) to service the entire array. Figure 3 shows an abstract block diagram of the inter-processor architecture; the DSP on each chassis now samples the 6 vibrissa (using the on-chip peripheral ADC module) and computes the IIR filtering of the FSC model. The filtered mechanical variables (16 bit) from each chassis are passed, via separate SPI buses, to the FPGA, which updates all 720 mechanoreceptor models and sends the resultant spike trains to the `brain stem' using a single SPI bus. The brainstem model has been implemented on a matrix of real-time spiking neural network processor FPGAs [3].

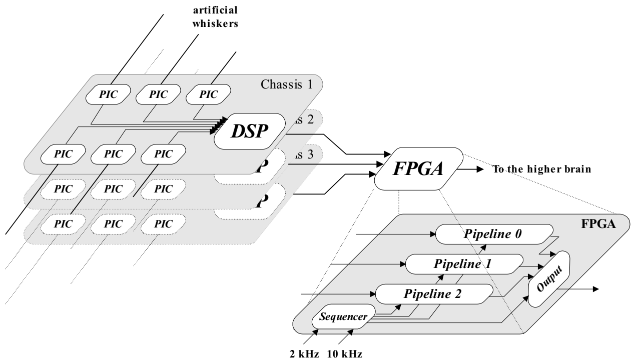

Figure 3: Block diagram of the inter-processor architecture.

3.3 The "MechanoProcessor"

The central FPGA modelling all 720 mechanoreceptors has been named the MechanoProcessor (see inset of Figure 3). It consists of a main sequencer module, 3 Mechanoreceptor Processing Elements (MPE) (each of which incorporates an SPI input bus) and a single SPI output module. The internal update period of the processor is 100µS to match the DSP sample rate, whilst the output update period is 500µS to synchronise with the 2KHz neural processors modelling the brain stem. The sequencer module, therefore, requires 2 separate synchronisation lines, 10 KHz and 2 KHz, in order to correctly coordinate the activity of the various concurrently operating modules of the system. Due to the high work demand of this application, the system has been designed to maximise the utility of the available hardware at all times. This has been accomplished using 3 main techniques:

3.3.1 FPGA Built in Functionalities

The Virtex II series of FPGAs from Xilinx [13] offer a wide range of built in functionalities such as up to 40 dedicated high speed 18bitsx18bits parallel multipliers (MULT18), which can be clocked at more than 200 MHz when pipelined, blocks of true dual port RAM of 18 Kbits (BRAM) with up to 3Mbits per device, distributed RAM in each configurable logic block (CLB) and digital clock management modules (DCM) to name only these. In order to provide a significant reduction in 'real-estate' requirements, both the FPGA dedicated multipliers and block RAMs have been adopted when designing the Mechanoprocessor. As there is always a cost to be paid, the design in this case is somehow hardware specific, and as such it will only work when targeting a limited range of FPGAs from the Xilinx's Virtex-II family, limiting thus its portability.

3.3.2 Pipelining the MPE

The individual MPEs have been designed using pipelining techniques to facilitate the parallel operation of as much of the FPGA hardware as possible thus maximising the throughput of the system. At MPEs level, pipelining means that the various stages of the mechanoreceptor model, detailed in Figure 2, are actually implemented as separate functional components. Each component receives its input from the previous component, processes it and passes the result to the next component in the pipeline. When the pipeline is fully loaded, each component will be working concurrently on a small part of the overall update algorithm of each mechanoreceptor resulting in maximum hardware utility and a minimum update time period.

3.3.3 Pipelining the Processor

To maximise the utility of the hardware, the entire processor system has been designed to operate as a pipeline itself, allowing all modules to operate concurrently whilst utilising a switched dual memory protocol to maintain data integrity between modules. This is achieved by introducing a fixed pipeline delay to the overall system. An example of an operational iteration of the MechanoProcessor is as follows (it is worth noting that each of the modules are operating concurrently which is not reflected in the sequential nature of the list):

i. The SPI module in each MPE reads data sent from the DSP on the corresponding sensor chassis and stores this information into local input RAM (RAM[0]).
ii. The first functional component of each MPE sequentially reads the data stored in local input RAM[1], channelling the results on through the rest of the pipeline.
iii. The last component of each MPE passes its results to an arbitrated central output RAM[0] which is local to the output SPI module.
iv. Every fifth internal update period (500µS, to synchronise the 10KHz MechanoProcessor to the 2 KHz brain stem model) the output SPI module reads data from output RAM[1] and sends this onto the brain stem model.
v. When all modules have completed an operational iteration and the next synchronisation trigger is received, the memories are switched such that the SPI input modules now write into local input RAM[1], the MPEs read from local input RAM[0] and write to global output RAM[1] and the output SPI module reads from output RAM[0].

This system introduces a propagation delay of one update period between modules, two between the input and output of the overall processor. The advantage gained by having all modules working continuously throughout each update period is that the utility of the available hardware is maximised, again increasing the overall throughput of the system. The contents of the currently write enabled output RAM block of the output SPI module, is updated by OR'ing the current state of each element with the corresponding new value from the MPEs during each internal update period (100µS). Therefore, any spikes that are initiated by a mechanoreceptor during the 500µS update period of the output module are latched. This reduction in resolution at the output is necessary to synchronise the high frequency peripheral neural processing with the lower frequency neural modelling in the brain stem. The PAs modelled in this system will never actually fire faster than 2KHz so there is no danger of a loss of data using this approach. Simulations of the hardware MechanoProcessor have demonstrated that it can update all 720 mechanoreceptors in 100µS. The SPI interface between each DSP and the MechanoProcessor has been implemented and demonstrated robustly transfer ring data at a rate of 5Mbps. The SPI between the MechanoProcessor and the brain stem neural processing based FPGA has also been demonstrated transferring data, accurately, at 5Mbps. Therefore, the bandwidths of all inter chip communications channels can comfortably accommodate the required data transfer rates demanded of the system.

4. RESULTS AND DISCUSSION

Simulations of the MechanoProcessor were undertaken to verify the algorithmic accuracy and the update period of the system. The input stimulus for these simulations were read from a file using a software interface instead of the SPI bus. These simulations demonstrated that the MechanoProcessor could accurately update all 720 mechanoreceptor models in the required 100μS update period. The DSP based mechanical model of the FSC was tested by using a function generator supplying a square wave to the ADC module. This represented an idealised strain profile of an artificial whisker making contact with an object during protraction of a whisk cycle (rising edge), maintaining contact for the duration of the protraction phase (plateau) and releasing contact during the retraction phase (falling edge). To constrain this strain profile to a single degree of freedom, i.e., no y-component, the ADC channel representing the y-axis of the imaginary vibrissae was held at VREFLOW whilst driving the x-axis channel with the square wave. Some example results from these tests are displayed in the plots of Figure 4. Similar tests were also conducted at the FPGA side of the SPI bus to verify that the MechanoProcessor was receiving the correct data. To test a hardware implementation of the MechanoProcessor, an XC2V3000 FPGA, located on a Celoxica RC203 development board, was used. The DSP was connected to the appropriate pins of the break-out header of the RC203 board and both systems were synchronised using a simple pulse generator located on the same FPGA. An RS232 serial interface was also instantiated on the FPGA which can broadcast 32 of the generated mechanoreceptor spike trains in real-time. A square wave signal was again applied to the ADC module of the DSP and the resultant spike trains generated by the MechanoProcessor were sampled using a PC. The MEAs of each mechanoreceptor pair (SA and RA) were uniformly distributed around the FSC, i.e., displaced by 180^o intervals (SA neural index 0 having an MEA of 0^o, whilst neural index 10 has an MEA of 180^o). The Figure showing the simulated results has been omitted for lack of space).

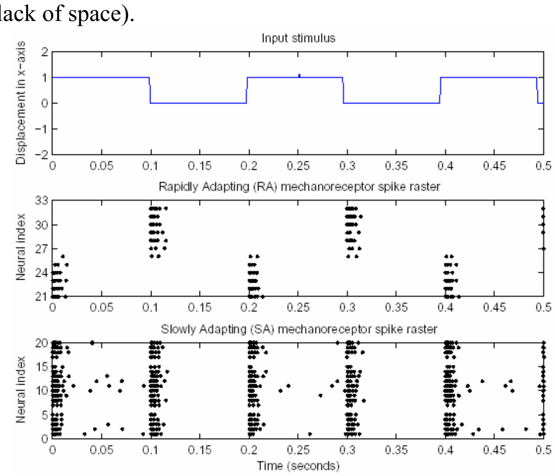

Figure 4: Spike output from 32 mechanoreceptors of a single FSC model in response to a square wave input. Data sampled at 2KHz.

The simulation has shown that SA mechanoreceptors are not as directionally sensitive to stimulus as the RA mechanoreceptors. There is, however, a higher spike activity in SA mechanoreceptors which have MEAs aligned with and 180^o to the direction of the input strain vector. The presence of spike activity in the SAs most aligned to the stimulus during the plateau phase of the artificial whisk cycle highlights the observation that certain cells are responsive throughout contact duration. The RA mechanoreceptors are much more directionally sensitive with minimal activity during the simulated plateau phase. Contact is indicated by strong responses in the RAs aligned with the direction of input strain vector whilst release is indicated by an equally strong response in those with opposing MEAs.

5. CONCLUSION

A biologically inspired tactile sensory system for neuromorphic signal processing applications has been designed and implemented. To test the model, a hardware implementation of the system using both DSP and FPGA processors has been carried out. The system has been demonstrated reproducing biologically plausible spike trains form a large number of primary afferents, which will be passed to a model of the brainstem for further processing and feature extraction. This will ultimately make a part of complete neuromorphic sensory system that will be ported on a mobile robot to carry a variety of real word tasks such as wall following, object recognition and surface texture discrimination.

6. REFERENCES

[1] G. Carvell and D. Simons, “Task and Subject Related Differences in Sensorimotor Behaviour During Active Touch," Behavioural Brain Research, Vol. 12, N°. 1, pp. 1 -9, 1995.

[2] The whiskerbot project." online at www.whiskerbot.org.

[3] M. J. Pearson, I. Gilhepsy, K. Gurney, C. Melhuish, B. Mitchinson, M. Nibouche and A. Pipe, “ Design and FPGA implementation of an embedded real time biologically plausible spiking neural network”, FPL’05, Helsinki, Finland 2005.

[4] R. Russel, “Using tactile whiskers to measure surface contours”, Proceedings of the IEEE Int. Conf. on Robotics and Automation, pp 1295 – 1299, 1992.

[5] M. Kaneko, N. Kanayama, and T. Tsuji, “Active Antenna for Contact sensing”, IEEE Trans. on Robotics and Automation, Vol. 14, N° 2, pp 278 – 291, 1998.

[6] J. L. Krichmar. and G. M. Edelman, ”Brain-based Devices for the Study of Nervous Systems and the Development of Intelligent Machines. Artificial Life, Vol. 11, pp 63 – 77, 2005.

[7] M. J. Pearson, I, Gilhespy, K. N. Gurney, C. Melhuish, B. Mitchinson, M. Nibouche, A. G. Pipe, T. J. Prescott and P. Redgrave, “A Biologically Inspired Haptic Sensor Array for use in Mobile Robotic Vehicles”, TAROS, London, Sep. 2005.

[8] A. Seth, J. McKinstry, G. Edelman and J. Krichmar, “Texture Discrimination by an Autonomous Mobile Brain-Based Device with Whiskers”, In Proc. ICRA2004, pp 4295 – 4930, 2004.

[9] M. Fend, S. Bovet, and V. Hafner, “The Artificial Mouse - a Robot with Whiskers and Vision, “In Proc. ISR 2004, 2004.

[10] Brecht, M., Preilowski, B., and Merzenich, ”Functional architecture of the mystacial vibrissae”, Behavioural Brain Research, Vol 84, pp 81-97, 1997.

[11] D. Kleinfeld, R. berg and S. O’Connor, “Anatomical Loops and Their Dynamics in Relation to Whisking by Rats”, Somatosensory and Motor Res. Vol. 16, No 2, p. 69-88, 1999.

[12] B. Mitchinson, K. Gurney, P. Redgrave, C. melhuish, A.G. Pipe, M. Pearson, I. Gilhespy and T. Prescott, “Empirically Inspired Simulated Electro-Mechanical Model of the Rat Mystacial Follicle Sinus Complex”, Proc. Roy. Soc, Biol. Sci., Vol. 271, pp 2509-2516, 2004.

[13] www.xilinx.com.